Shape and Size Control of Regularly Arrayed Nanodots Fabricated Using Ultrathin Alumina Masks

Yong Lei*,†,‡ and Wai-Kin Chim‡,§

Institut für Nanotechnologie, Forschungszentrum Karlsruhe, Karlsruhe, Germany 76021, and Singapore-MIT Alliance and Department of Electrical and Computer Engineering, National University of Singapore, 4 Engineering Drive 3, Singapore 117576

Received August 19, 2004

We report an approach to fabricate highly ordered semiconductor and metal nanoparticle arrays with controllable shapes and sizes, including nanometer-sized disks, hemispheres, hemiellipsoids, and conics. The nanoparticle arrays are fabricated on Si and Si/SiO_2 substrates using ultrathin alumina masks (UTAMs) as evaporation masks. The shapes and the sizes of the nanoparticles are adjusted by changing the aspect ratio of the apertures of the UTAMs, and the amount of material deposited through the UTAMs. Highly ordered semiconductor nanoparticle arrays with particle sizes down to about 20 nm have also been fabricated.

Introduction

In many applications of nanostructured materials, such as microelectronics, optoelectronics, and sensing, the ability to fabricate nanostructures with a high degree of regularity and uniformity is important in achieving tight control of their properties. Depending on the material, different nanostructure fabrication techniques are generally required. The template method[1−16] is one commonly used approach to obtain ordered arrays of one-dimensional nanostructures. As a well-established nanotemplate, porous anodic alumina has been widely used to fabricate many kinds of nanowires[1−13] and nanotubes,[13−15] especially after the great improvement in pore regularity achieved using a two-step anodization process as proposed by Masuda.[16] Other methods for fabricating ordered arrays include electron beam lithography,[17,1817−18] nanoimprint,[19] and self-assembly processes.[20,21] However, there are fabrication and application restrictions for these methods, such as limited pattern area and low throughput, high equipment capital costs, and limited classes of materials that can be fabricated. In comparison, template methods are much cheaper, and can be used to pattern large areas (several tens of square centimeters) of surfaces. Additionally, template methods allow for deposition of a wide range of materials.[1] Recently, through the use of ultrathin alumina masks (UTAMs) as evaporation masks, large-scale ordered metal nanoparticle arrays have been fabricated with relatively low equipment cost.[16,22−27] The process involves the successful transfer of the regularity of the pore arrays of the UTAMs into the nanoparticle array. Moreover, initiated from the ordered catalyst metal nanoparticle arrays, highly ordered nanotube arrays have also been fabricated.[27] However, most works so far in the field are limited in the fabrication process. In addition, the sizes of the nanoparticles, which were in the range of 25−80 nm, can only be adjusted by changing the diameters of the pores of the UTAMs.

* To whom correspondence should be addressed. Tel: 49(0)7247-82-6779. Fax: 49(0)7247-82-6368. E-mail: yong.lei@int.fzk.de; yuanzhilei@yahoo.com.
† Institut für Nanotechnologie.
‡ Singapore-MIT Alliance.
§ Department of Electrical & Computer Engineering, National University of Singapore.

(1) Martin, C. R. *Science* **1994**, *266*, 1961.
(2) Masuda, H.; Yanagishita, T.; Yasui, K.; Nishio, K.; Yagi, I.; Rao, T. N.; Fujishima, A. *Adv. Mater.* **2001**, *13*, 247.
(3) Whitney, T. M.; Jiang, J. S.; Searson, P. C.; Chien, C. L. *Science* **1993**, *261*, 1316.
(4) Preston, C. K.; Moskovits, M. *J. Phys. Chem.* **1993**, *97*, 8495.
(5) Routkevitch, D.; Tager, A. A.; Haruyama, J.; Almawlawi, D.; Moskovits, M.; Xu, J. M. *IEEE Trans. Electron Devices* **1996**, *43*, 1646.
(6) Huber, C. A.; Huber, T. E.; Sadoqi, M.; Lubin, J. A.; Manolis, S.; Prater, C. B. *Science* **1994**, *263*, 800.
(7) Nielsch, K.; Muller, F.; Li, A. P.; Gösele, U. *Adv. Mater.* **2000**, *12*, 582.
(8) Xu, D. S.; Xu, Y. J.; Chen, D. P.; Guo, G. L.; Gui, L. L.; Tang, Y. Q. *Adv. Mater.* **2000**, *12*, 520.
(9) Lei, Y.; Zhang, L. D.; Meng, G. W.; Li, G. H.; Zhang, X. Y.; Liang, C. H.; Chen, W.; Wang, S. X. *Appl. Phys. Lett.* **2001**, *78*, 1125.
(10) Lei, Y.; Zhang, L. D.; Fan, J. C. *Chem. Phys. Lett.* **2001**, *338*, 231.
(11) Cao, H. Q.; Xu, Y.; Hong, J. M.; Liu, H. B.; Yin, G.; Li, B. L.; Tie, C. Y.; Xu, Z. *Adv. Mater.* **2001**, *13*, 1393.
(12) Sander, M. S.; Prieto, A. L.; Gronsky, R.; Sands, T.; Stacy, A. M. *Adv. Mater.* **2002**, *14*, 665.
(13) Lakshmi, B. B.; Patrissi, C. J.; Martin, C. R. *Chem. Mater.* **1997**, *9*, 2544.
(14) Hoyer, P. *Adv. Mater.* **1996**, *8*, 857.
(15) Li, J.; Paradopoulos, C.; Xu, J. M.; Moskovits, M. *Appl. Phys. Lett.* **1999**, *75*, 367.
(16) Masuda, H.; Satoh, M. *Jpn. J. Appl. Phys.* **1996**, *35*, 126.
(17) Pease, R. F. W.; Han, L.; Winograd, G.; Meisburger, W. D.; *Microelectron. Eng.* **2000**, *53*, 55.
(18) Chang, T. H. P.; Mankos, M.; Lee, K. Y.; Muray, L. P. *Microelectron. Eng.* **2001**, *57*, 117.
(19) Chou, S. Y.; Krauss, P. R.; Renstrom, P. J. *Appl. Phys. Lett.* **1995**, *67*, 3114. Chou, S. Y.; Krauss, P. R.; Renstrom, P. J. *Science* **1996**, *272*, 85.
(20) Puntes, V. F.; Krishnan, K. M.; Alivisatos, A. P. *Science* **2001**, *291*, 2115.
(21) Sun, S.; Murray, C. B.; Weller, D.; Folks, L.; Moser, A. *Science* **2000**, *287*, 1989.
(22) Masuda, H.; Yasui, K.; Nishio, K. *Adv. Mater.* **2000**, *12*, 1031.
(23) Cheng, G.; Moskovits, M. *Adv. Mater.* **2002**, *14*, 1567.
(24) Sander, M. S.; Tan, L. S. *Adv. Funct. Mater.* **2003**, *13*, 393.
(25) Wu, Z. H.; Mei, X.; Kim, D.; Blumin, M.; Ruda, H. E.; Liu, J. Q.; Kavanagh, K. L. *Appl. Phys. Lett.* **2003**, *83*, 3368.
(26) Hobbs, K. L.; Larson, P. R.; Lian, G. D.; Keay, J. C.; Johnson, M. B. *Nano Lett.* **2004**, *4*, 167.
(27) Lei, Y.; Yeong, K. S.; Thong, J. T. L.; Chim, W. K. *Chem. Mater.* 2004, *16*, 2757.

10.1021/cm048609c CCC: $30.25
Published on Web 01/13/2005

At nanometer length scales, many new phenomena and physical properties are closely related to the shape and size of the nanoparticles, and thus the ability to vary these parameters is a key to realizing nanostructures with novel properties. Anisotropic optical and magnetic properties have been found in metallic nanorods,[3−5,28,29] metallic nanoparticles,[30,31] and metallic nanodisks.[32] Also, the luminescence of cadmium selenide (CdSe) semiconductor nanorods[33] is strongly related to their shape. Nanoparticles of other shapes have also been fabricated, including cubic[34] and triangular[35] cadmium sulfide (CdS) and triangular silver nanodots.[36] Moreover, size is often a crucial nanostructure parameter. Some magnetic nanostructures show interesting properties as their size becomes comparable to certain lengths, such as the spin-flip diffusion length and magnetic domain-wall width.[37] For such reasons, good control of shape and size in nanoparticle fabrication has become one of the challenges in nanoscience and nanotechnology.

In this paper, we achieved shape and size tuning of highly ordered arrayed semiconductor (CdSe and CdS) and metal (Ni) nanoparticles on Si and Si/SiO_2 substrates, which were prepared using ultrathin alumina masks (UTAMs) as evaporation masks. By changing the aspect ratio of the apertures of the UTAMs and the amount of material deposited through the UTAMs, the shapes of the nanoparticles can be adjusted from nanometer-sized disks, to hemispheres and hemiellipsoids, and finally to conics. The sizes of the nanoparticles can be adjusted simultaneously with appropriate shape control. Semiconductor nanoparticle arrays with particle sizes as small as 20 nm were also fabricated.

Experimental Section

The entire fabrication process of UTAMs and highly ordered nanoparticle arrays is outlined in Figure 1.

Fabrication of UTAMs on Si and Si/SiO_2 Substrates (Figure 1a−f). The ultrathin anodic alumina masks we used were prepared in a two-step anodization process.[16] High-purity (99.99+%) aluminum foil of about 0.22-mm thickness was used as the starting material. Before anodization, the aluminum foil was first degreased with acetone, and then annealed at 400 °C for 4 h under vacuum conditions to remove mechanical stresses; finally, it was electropolished in a 1:9 solution of perchloric acid and ethanol. After the first anodization step (Figure 1a), the anodic oxide layer was removed in a mixture of H_3PO_4 (6 wt %) and H_2CrO_4 (1.8 wt %) at 60 °C (Figure 1b). This specimen was anodized again for a very short time resulting in a very thin alumina layer (Figure 1c). The anodization conditions, including acid solutions and concentrations, voltage, temperature, second anodization duration, and thickness

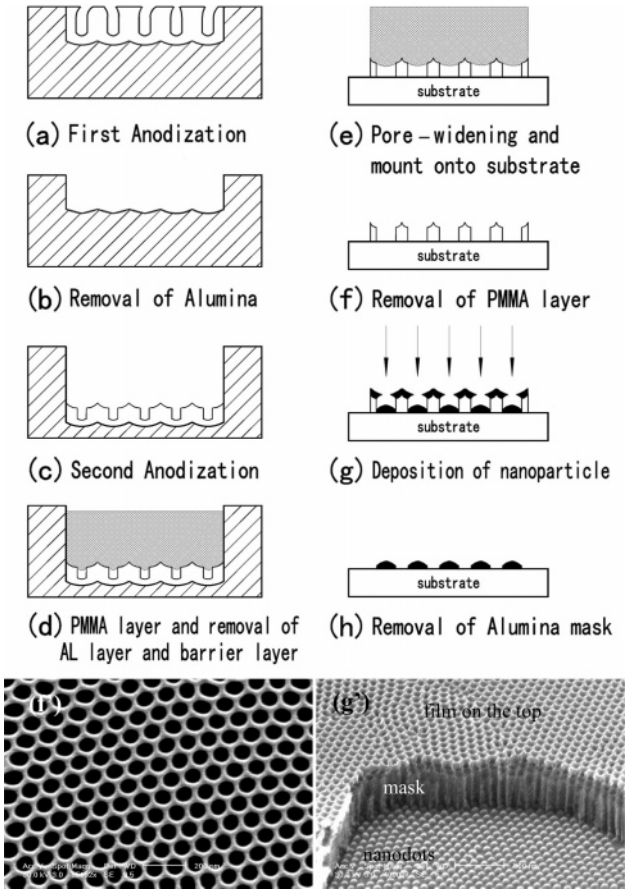

Figure 1. Schematic outline of the fabrication of highly ordered nanoparticle arrays (a)−(h); (f′) and (g′) are SEM images of the products in procedure (f) and (g). (f′) Top view of the UTAM prepared in 0.3 M oxalic acid solution at 17 °C and anodization voltage of 40 V (pore diameter and cell size of the UTAM are about 80 and 105 nm, respectively). (g′) CdS nanoparticle arrays with part of the UTAM remaining.

of the alumina layer, are stated in the respective figure captions. A PMMA layer was then deposited on the top of the alumina layer from a 6% PMMA/chlorobenzene solution, and baked at 120 °C for about 25 min (Figure 1d). After that, the Al layer was removed in $SnCl_2$ solution. The removal of the barrier layer and the following pore-widening process was carried out in 5 wt % H_3PO_4 solution, forming an ultrathin alumina mask (UTAM) with a PMMA layer on the top. Then the UTAM/PMMA was mounted on the respective substrates (Si and Si/SiO_2) (Figure 1e). The PMMA layer was removed using acetone or chloroform (Figure 1f). The top surface of a typical UTAM prepared in 0.3 M oxalic acid solution at 40 V in 17 °C is shown in Figure 1f′. The pore regularity is extremely good as it arises from a long first anodization duration of 10 h. The area of the UTAM can be as large as several tens of square centimeters.

Preparation of Highly Ordered Nanoparticle Arrays. CdS, CdSe, and Ni were thermally evaporated using an Edwards Auto 306 Evaporator (Figure 1g); the vacuum is about 5 microTorr while the evaporation rate is about 0.2−0.3 nms^{-1}. After the preparation of the nanoparticles, the UTAMs were removed by simply immersing the samples in acetone for 1−2 min followed by a rinse with DI water, leaving the highly ordered nanoparticle arrays on the surface of the substrate (Figure 1h).

Characterization. Structures of the fabricated UTAMs and nanoparticle arrays were observed using a scanning electron microscope [(SEM), Philips XL-30 FEG] and an atomic force microscope [(AFM), Digital Instruments Dimension 3000]. All AFM measurements were carried out under tapping-mode operation.

(28) Yu, Y. Y.; Chang, S. S.; Lee, C. L.; Wang, C. R. C. *J. Phys. Chem. B* **1997**, *101*, 1588.
(29) Jana, N. R.; Gearheart, L.; Murphy, C. J. *Chem. Commun.* **2001**, 617.
(30) Porto, M. *J. Appl. Phys.* **2002**, *92*, 6057.
(31) Batlle, X.; Labarta, A. *J. Phys. D: Appl. Phys.* **2002**, *35*, R15.
(32) Maillard, M.; Giorgio, S.; Pileni, M. P. *Adv. Mater.* **2002**, *14*, 1084.
(33) Hu, J.; Li, L.; Yang, W.; Manna, L.; Wang, L.; Alivisatos, A. P. *Science* **2001**, *292*, 2060.
(34) Chen, C. C.; Lin, J. J. *Adv. Mater.* **2001**, *13*, 136.
(35) Pinna, N.; Weiss, K.; Urban, J.; Pileni, M. P. *Adv. Mater.* **2001**, *13*, 261.
(36) Jin, R.; Cao, Y.; Mirkin, C. A.; Kelly, K. L.; Schatz, G. C.; Zheng, J. G. *Science* **2001**, *294*, 1901.
(37) Awschalom, D. D.; von Molnar, S. In *Nanotechnology*; Timp, G., Ed.; Springer: New York, 1999; Ch. 12.

To improve the resolution of the AFM images of the nanoparticles, especially in the size-range of 20−100 nm, we used high-aspect-ratio TESP probe tips (from Veeco Instruments, Inc.) in all the AFM measurements. The radius of the curvature of the tip end is less than 5 nm.

Results and Discussion

Figure 1g′ shows a typical sample of highly ordered nanoparticle arrays (CdS) on Si wafer, where part of the UTAM is left behind intentionally. The size distribution of the arrayed nanoparticles is highly monodisperse. Besides the nanodots at the bottom of the apertures, there is a sieve-like layer at the top of the pore walls of the UTAM.[26,27] At the beginning of the deposition process, the pores of this top layer have a diameter similar to that of the pores of the UTAMs. As the deposition progresses, the pores of the top layer shrink continuously and finally result in the closure of the pores and termination of the nanoparticle growth. This is the closure effect in the growth process of the nanoparticles using UTAM as the evaporation mask.[27]

The following analyses of the shape and size control of the nanoparticles were performed using four different UTAMs, which were prepared in oxalic acid solution under almost identical conditions, except for different second anodization durations that resulted in different thicknesses of the UTAMs. The cell sizes of these UTAMs are about 105 nm and the pores were widened to about 80 nm. The aspect ratios of the apertures of the four UTAMs are approximately 1:2, 1:3, 1:4, and 1:8. The thicknesses of the corresponding deposited materials using these UTAMs are 1.5 nm (Figure 2), 35−40 nm (Figure 3), 50−55 nm (Figure 4), and 60 nm (Figure 5), respectively. The fabricated nanostructure dimensions were measured using SEM, and further verified and characterized using AFM section analysis to show their respective shapes.

Nanodisks. By using a 1:2 aspect ratio UTAM (shown in the inset of Figure 2a) and a relatively thin nickel (Ni) deposited layer of about 1.5 nm, a nanodisk array was obtained (Figure 2a). The cross-sectional AFM profile of 5 nanoparticles is shown in Figure 2b, which clearly shows the disklike feature of the nanoparticles. The two cursors in Figure 2b are located at the center and the edge of a nanodisk, thus the vertical distance (1.465 nm) in the parameter table is actually the estimated thickness of the nanodisk. Because the end of the AFM tip cannot be prefectly sharp and there is a finite curvature even for high-aspect-ratio probe tips, the size of the nanoparticles obtained from the AFM measurement is slightly larger than the actual size, especially for nanoparticles with relatively steep edges. Therefore, the estimated diameter of the nanodisk is about 80 nm, which is about 4−5 nm smaller than the measured AFM value (84.228 nm, which is twice the horizontal distance in the parameter table). The estimated diameter of the nanodisks of about 80 nm and the spacing between the adjacent nanodisks of about 105 nm, are in good agreement with the pore diameters and cell sizes of the UTAM.

Because the thickness of the nanodisks (about 1.5 nm) is quite small when compared to their diameter of about 80 nm, we did not use the same dimension scale for the horizontal and vertical coordinates in the cross-sectional AFM profile plot. The actual shape of the nanodisks should be much flatter than that in the cross-sectional profile in Figure 2b.

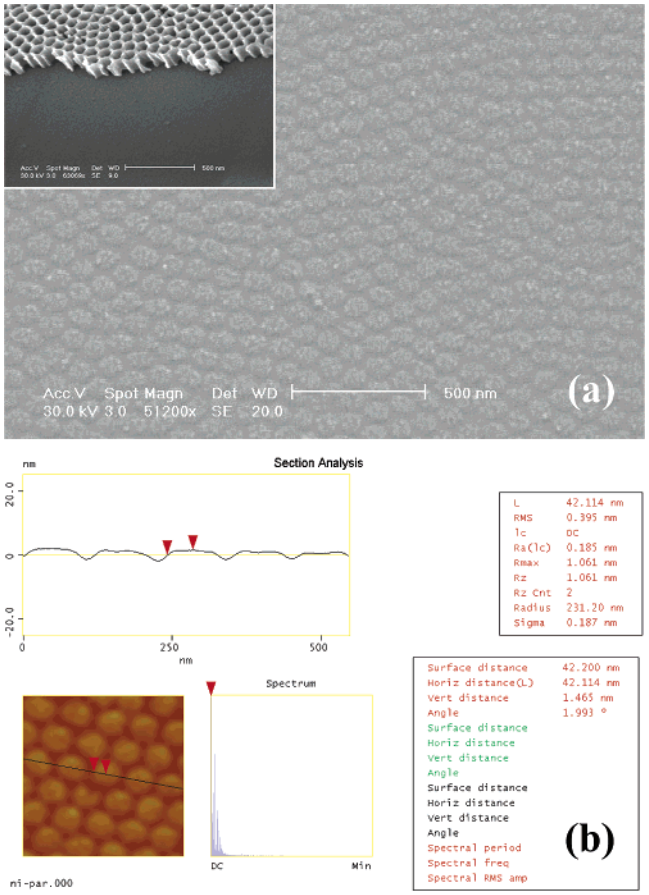

Figure 2. Highly ordered nanodisk arrays (Ni). (a) SEM image of the nanodisks. The inset in (a) shows the corresponding UTAM used in the fabrication process. Pore diameter, cell size, and thickness of the UTAM, which was prepared in 0.3 M oxalic acid solution at 17 °C and anodization voltage of 40 V for 100 sec, are about 80, 105, and 160 nm, respectively. The aspect ratio of the apertures of the UTAM is about 1:2. (b)AFM section analysis of the nanodisks in (a); the average height and size of the nanodisks are approximately 1.5 and 80 nm, respectively.

Nanohemispheres. When the aspect ratio of the UTAM apertures was increased from 1:2 to 1:3 (inset of Figure 3a) and with a thicker deposited layer of about 35−40 nm, the arrayed nanoparticles (CdSe) had a hemispherical shape (Figure 3a). To accurately reflect the shape of the nanoparticles, we used the same dimension scale for the horizontal and vertical coordinates in the cross-sectional AFM profile plot in Figure 3b (also in the following Figures 4b and 5b). Figure 3b clearly shows that the particles are hemispheres with height and base diameters of about 35−40 and 75 nm, respectively. The diameters of the hemispheres are slightly smaller than those of the nanodisks in Figure 2.

Nanohemiellipsoids. With further increase of the aspect ratio to 1:4 (inset in Figure 4a) and a much thicker deposited layer of about 50−55 nm, the nanoparticles (CdS) become taller hemiellipsoids with even smaller base diameters of about 65 nm. The cross-sectional AFM profile in Figure 4b clearly shows the shapes of the hemiellipsoids with average height and base diameters of about 50−55 and 65 nm, respectively.

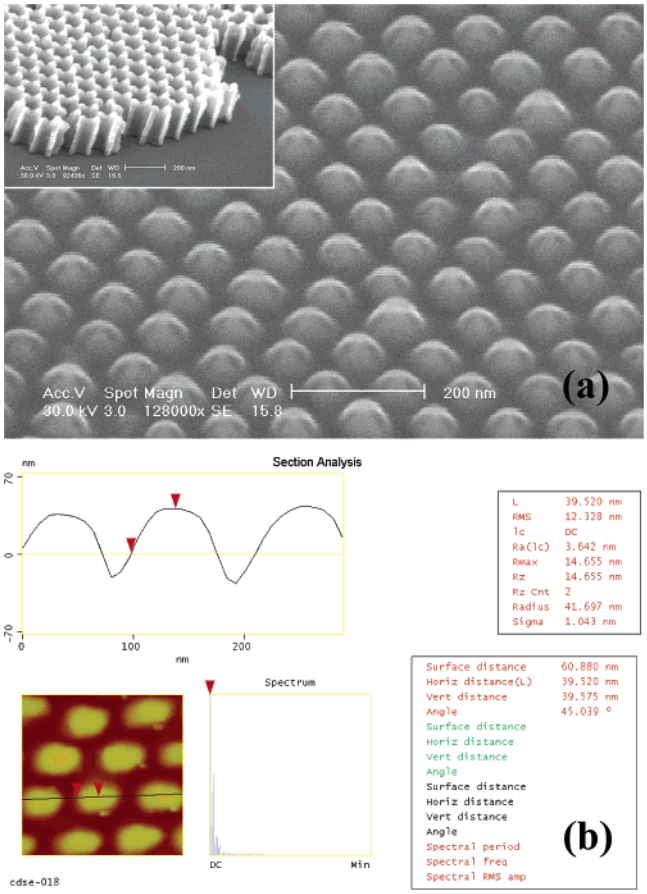

Figure 3. Highly ordered nanohemisphere arrays (CdSe). (a) SEM image of the nanohemispheres. The inset in (a) shows the corresponding UTAM used in the fabrication process. Pore diameter, cell size, and thickness of the UTAM, which was prepared in 0.3 M oxalic acid solution at 17 °C and anodization voltage of 40 V for 2.5 min, are about 80, 105, and 240 nm, respectively. The aspect ratio of the apertures of the UTAM is about 1:3. (b) AFM section analysis of the nanohemispheres in (a); the average height and base diameter of the nanohemispheres are approximately 35-40 and 75 nm, respectively. In the section analysis, to accurately reflect the shape of the nanoparticles, we used the same dimension scale for the horizontal and vertical coordinates.

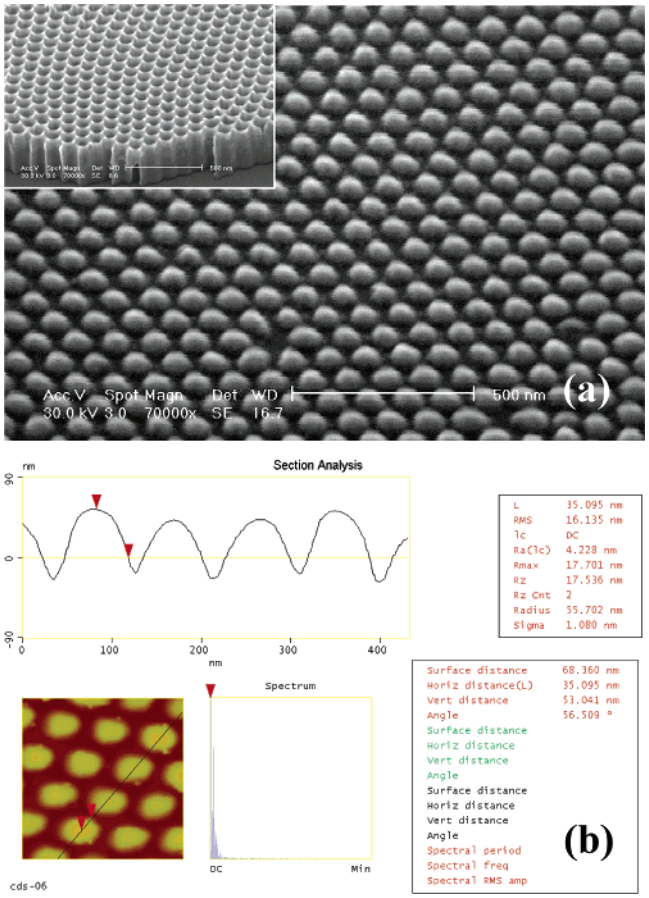

Figure 4. Highly ordered nanohemiellipsoid arrays (CdS). (a) SEM image of the nanohemiellipsoids. The inset in (a) shows the corresponding UTAM used in the fabrication process. Pore diameter, cell size, and thickness of the UTAM, which was prepared in 0.3 M oxalic acid solution at 17 °C and anodization voltage of 40 V for 3.5 min, are about 80, 105, and 310 nm, respectively. The aspect ratio of the apertures of the UTAM is about 1:4. (b) AFM section analysis of the nanohemiellipsoids in (a); the average height and base diameter of the nanohemiellipsoids are approximately 50−55 and 65 nm, respectively. In the section analysis, to accurately reflect the shape of the nanoparticles, we used the same dimension scale for the horizontal and vertical coordinates.

Nanoconics. When the aspect ratio was finally increased to 1:8 with a deposited layer of greater than 60 nm thickness, the tops of the nanoparticles (CdSe) became quite sharp and nanometer-sized conics were obtained (Figure 5a and its inset). The cross-sectional AFM profile in Figure 5b clearly shows the conical shape of the nanoparticles with average height of about 55−60 nm. The base diameters of the particles further decrease to about 60 nm. The nanoparticles in the AFM images in Figures 3b, 4b, and 5b are slightly elongated. This artifact is caused by the scan direction of the TESP probe tip in relation to the orientation of the nanoparticles and is usually observed in the AFM characterization of nanometer-sized arrayed particles, especially when the nanoparticles are relatively thick and not tightly fixed to the substrates.

As the aspect ratio of the apertures of the UTAMs changes from 1:2 to 1:8, and the thickness of the deposited layer changes from 1.5 nm to greater than 60 nm, the shape of the nanoparticles changes from disks to hemispheres and hemiellipsoids, and finally to conics. Correspondingly, the base diameter of the nanoparticles decreases from 80 to 75 nm and 65 nm, and finally to 60 nm while maintaining the same spacing between the adjacent nanoparticles of about 105 nm.

Mechanism of the Shape and Size Tuning. Figure 6 is a schematic outline of the shape and size adjustment of nanoparticles by changing the aspect ratio of the apertures of the UTAMs and the amount of material deposited through the UTAMs. The observed shape and size changes of the nanoparticles are thought to arise from the closure effect in the evaporation process and also originated from the shadowing effect of the UTAMs.

Closure Effect. As mentioned above, at the beginning of the deposition there is a top layer formed on the UTAMs with pores similar to pores of the UTAMs (Figure 6a). Therefore, nanoparticles with flat top surfaces, disk-shaped nanoparticles, are obtained. With the deposition progresses, there is a closure effect of the pores of the top layer which will lead to the continuous shrinkage of the aperture size.[27] This closure effect sharpens the top of the nanoparticles gradually, resulting in hemispherical-shaped particles (Figure 6b) and then hemiellipsoids (Figure 6c). Further evaporation will clog the pores, resulting in conical-shaped nanoparticles (Figure 6d).

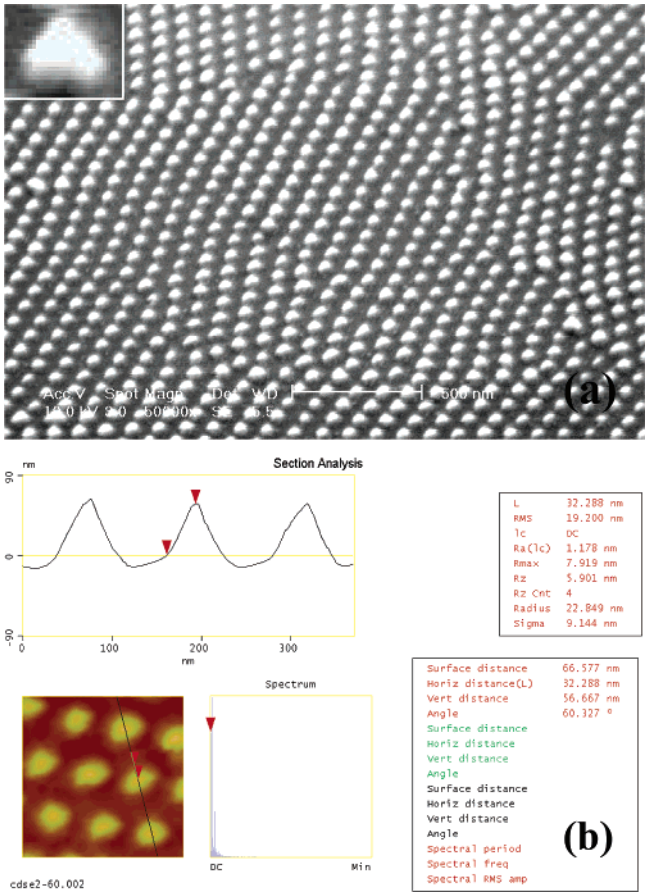

Figure 5. Highly ordered nanoconic arrays (CdSe). (a) SEM image of the nanoconics. The inset in (a) is the enlarged image of a nanoconic. Pore diameter, cell size, and thickness of the UTAM used in the fabrication process, which was prepared in 0.3 M oxalic acid solution at 17 °C and anodization voltage of 40 V for 7 min, are about 80, 105, and 650 nm, respectively. The aspect ratio of the apertures of the UTAM is about 1:8. (b) AFM section analysis of the nanoconics in (a); the average height and base diameter of the nanoconics are approximately 55−60 and 60 nm, respectively. In the section analysis, to accurately reflect the shape of the nanoparticles, we used the same dimension scale for the horizontal and vertical coordinates.

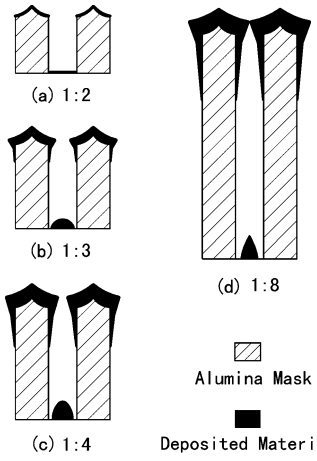

Figure 6. Schematic outline of the shape and size adjustment of nanoparticles by changing the aspect ratio of the apertures of the UTAMs and the amount of material deposited through the UTAMs. (a), (b), (c), and (d) correspond to the UTAMs and nanoparticles in Figures 2, 3, 4, and 5, which are nanometer-sized disks, hemispheres, hemiellipsoids, and conics, respectively.

Shadowing Effect. It is known that the channels of the UTAMs are unlikely to be perfectly smooth cylinders that are perpendicular to the substrate. Corrugations along the channel give rise to shadowing, especially when the aspect ratio of the channels is high. Moreover, it is usually impossible to achieve a perfect parallel between the evaporation direction and the channels of the UTAMs. This also enhances the shadowing effect of the pore walls to the deposited materials. The shadowing effect results in the attachment of the deposited materials on the pore walls of the UTAMs,[26] and consequently causes the diameters of the nanoparticles to decrease as the aspect ratio of the pores is increased. When the aspect ratio is 1:2 (Figure 6a), the diameter of the nanodisks (about 80 nm) is similar to that of the UTAM pores, indicating that there is almost no shadowing for UTAMs of small aspect ratios. With the aspect ratio of the UTAM increasing to 1:3 and 1:4, the base diameters of the nanoparticles decrease to about 75 and 65 nm (Figure 6b and c, respectively), and this is caused by the shadowing effect of the UTAMs. Enhanced shadowing

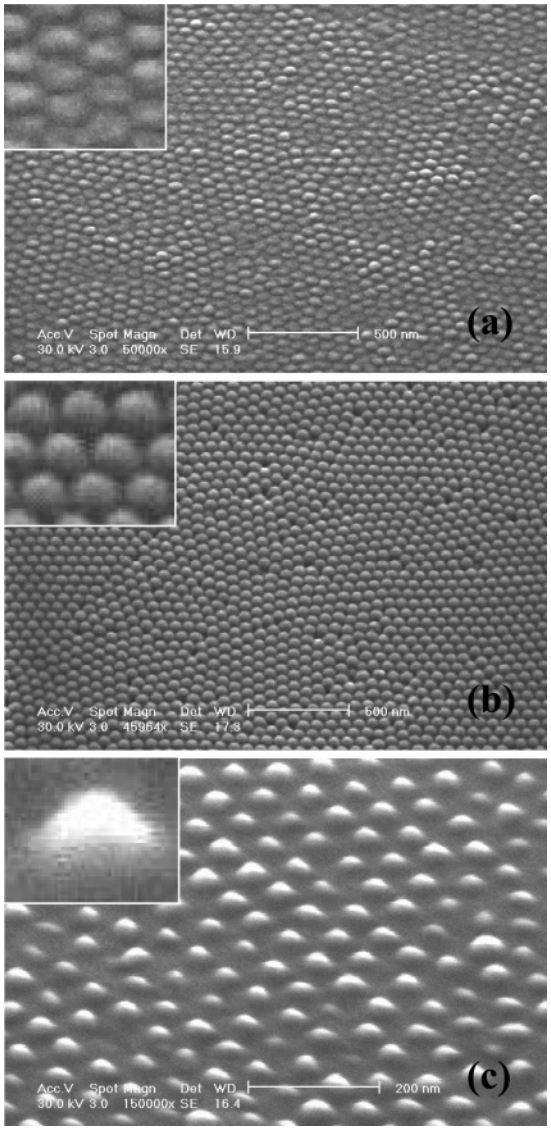

Figure 7. Highly ordered nanoparticle arrays with small diameters (CdSe): nanodisks (a), nanohemispheres (b), and nanoconics (c). The UTAMs used in (a), (b), and (c), which were prepared in 0.3 M sulfuric acid solution at 0 °C and anodization voltage of 27 V, have the same pore diameter and cell size of about 45 and 66 nm, respectively. The aspect ratios of the apertures of the UTAMs are different, which are about 1:3 (a), 1:4 (b), and 1:10 (c). The base diameters are approximately 45 nm (a), 40 nm (b), and 20-40 nm (c), respectively.

effect was observed when the aspect ratio increased to 1:8, which resulted in the 60-nm base diameter of the nanoparticles (Figure 6d). The shadowing effect may also affect the shapes of the nanoparticles with the change in aspect ratios of the UTAMs.

Shape and Size Control of Arrayed Nanoparticles with Small Sizes. Nanoparticle arrays fabricated using another set of UTAMs with smaller pore diameters confirms the above shape and size trends (Figure 7). The UTAMs were fabricated in sulfuric acid solution with cell sizes of about 66 nm and pore diameters of about 45 nm. The aspect ratios of the apertures of the UTAMs are about 1:3 (a), 1:4 (b), and 1:10 (c). The shape of the CdSe nanoparticles changes from disks (a), to hemispheres (b), and finally to conics (c), similar to previous results from UTAMs with larger pore diameters. The base diameters also decrease from 45, to 40, and finally to 20−40 nm. Some conics are smaller than 20 nm (Figure 7c).

Discussion. Highly ordered metal and semiconductor nanoparticle arrays, with controllable shapes and sizes, should have wide potential applications, such as in magnetic, optical, and microelectronic devices. The nanometer-sized disk and conic arrays, such as optical semiconductors (CdS and CdSe) materials and magnetic metal (Ni) materials, should be suitable for studying optical and magnetic anisotropies. Such conic arrays with sharp ends may also have potential application in electron emitter arrays.[38]

As mentioned above, with the same UTAM pore diameter, the particle size can also be changed by varying the aspect ratio of the apertures. Therefore, apart from changing the anodization voltage and acid solutions to adjust the cell sizes and pore diameters of the UTAMs, and consequently the planar size of deposited nanoparticles,[27] the pore-widening process together with the thickness of the UTAMs (aspect ratio of the apertures) can also change the planar size and the interparticle spacing of the nanoparticles. The ability to independently adjust the interparticle spacing without changing the pitch is very useful in studying the interaction between adjacent nanoparticles in the nanoparticle array.

We have also fabricated highly ordered nanoparticle arrays of other materials using the same method, including Au, In, Sn, Fe, and Ge with thermal and electro-beam evaporation and sputtering, and found that the shape and size trend changes are the same as those of the Ni, CdSe, and CdS nanoparticles in this article. This implies that the shape and size control of the arrayed nanoparticles are independent of the materials deposited. This demonstrates the general utility of the approach in fabricating many kinds of nanoparticles with controllable shapes and sizes.

Conclusions

In conclusion, highly ordered semiconductor and metal nanoparticle arrays have been successfully fabricated using ultrathin alumina membranes as evaporation masks. By changing the aspect ratio of the apertures of the UTAMs and the amount of deposited material through the UTAMs, it is possible to tune the shapes and sizes of the nanoparticles, to give nanometer-sized disks, hemispheres, hemiellipsoids, and conics. The technique reported here for the shape and size control of the arrayed nanoparticles should be a general approach to fabricate many kinds of nanoparticles with tunable shapes and sizes.

Acknowledgment. We thank Shuwen Zhang for the drawing preparation and J. T. L. Thong for valuable discussion. Y. Lei is grateful for the research fellowship from the Alexander von Humboldt Foundation and the Singapore-MIT Alliance.

CM048609C

(38) Spindt, C. A.; Brodie, I.; Humphrey, L.; Westerberg, E. R. *J. Appl. Phys.* **1976**, *47*, 5248.